A Novel Current Control Method of a Three-Leg Inverter in the Stationary Frame for a Two-Phase AC Motor

Yixiao Luo, Dezhi Chen, Byung-il Kwon
Department of Electronic Systems Engineering,
Hanyang University
Ansan, Korea
yxluowhu@hotmail.com, chendezhi_1934@126.com,
bikwon@hanyang.ac.kr

Thomas Anthony Lipo
Department of Electrical & Computer Engineering,
University of Wisconsin-Madison
Madison WI, USA
thomas.lipo1@gmail.com

***Abstract*—This paper proposes a novel method to control the current of a three-leg voltage source inverter (VSI) supplying a two-phase induction motor (TPIM) in the stationary frame by modulating the potential of neutral leg middle point with a proposed algorithm and using two closed loops with optimized proportional and resonant (PR) controllers to regulate the current. Two conventional current control strategies for conventional three-leg VSI in the stationary frame are presented. Then the novel control method is introduced. Both computer simulation and experiment results show the effectiveness of the proposed method in achieving better performance in terms of total harmonic distortion (THD), peak overshoot value of output current.**

Keywords—DC/AC converter; current control; stationary frame;

I. INTRODUCTION

The permanent split-capacitor motor (PSCM) is the most common form of a typical two-phase machine, also recognized as the single-phase induction motor (SPIM) [1], [2], [3] which is widely used and intensely researched. By removing the capacitor of the SPIM, it turns into an asymmetrical, capacitorless two-phase induction motor (TPIM), which is selected as a model motor of this paper.

For supplying a TPIM, three different voltage source inverter topologies can be used, four-leg inverter, three-leg and two-leg inverter. The performance and open loop pulse width modulation (PWM) methods of these topologies have been analyzed in [4]. The three-leg inverter is selected here as the model inverter, since it costs less than a four-leg inverter and produces less harmonics than a two-leg inverter, of which the connection to a TPIM is shown in Fig. 1. Variable speed control and different modulation strategies of this topology supplying a TPIM has also been researched in [5], [6].

In some cases, motor currents rather than motor terminal voltages are directly commanded, such as for high performance drive systems, where precise current control is essential for precise torque or speed control. Current regulators can be categorized as linear PI, hysteresis and deadbeat predictive in

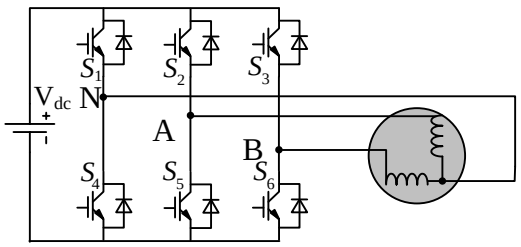

Fig. 1. Schematic diagram of an inverter.

stationary or synchronous frame [7]. Generally controllers in synchronous frame are supposed to have better performance than in the stationary frame since they act on DC quantities and it is then possible to achieve zero steady-state error. A double sequence controller to compensate the negative components caused by imbalanced load in synchronous frame is introduced in [8], [9]. However, it is quite complex to transform the stationary frame to the synchronous frame and then transform it back to stationary frame. Therefore, in this paper currents are regulated in the stationary frame to avoid the frame transformation. Though hysteresis control is proved to be effective, its high switching frequency causes losses and may damage the switches. Subsequently, it is determined to utilize a PR controller to regulate the AC current in stationary frame to achieve almost zero steady-state error [10]. Methods to improve the performance of current control in stationary frame including the optimization of PI, or proportional and resonant (PR) controllers and using feedforward compensation to eliminate the error caused by back electromotive force (EMF) disturbance have been proposed and examined in [11], [12].

A simple way to control the current of a three-phase load in stationary frame uses three PI controllers which can also be applied to the two-phase load system, named method I. Meanwhile another method of using only two PI controllers and from which the modulation signal for the third obtained, introduced in [13] also works for a two-phase load system, named method II. Furthermore, a novel current control algorithm modulating the potential of the middle point of the neutral leg to eliminate the error is proposed.

978-1-4673-7376-0/15/$31.00 ©2015 IEEE

All three methods are verified in MATLAB/SIMULINK, and compared in terms of total harmonic distortion (THD), peak overshoot. Also, an experimental prototype consisting of a microprocessor-based controller, the three-leg voltage source inverter, and a 0.75kW two-phase induction motor, is constructed to confirm the proposed control strategy of achieving better performance than the conventional methods.

II. Modelling, Control and Simulation

A. Modelling of a Two-phase Induction motor

The dynamic equations of a generic unsymmetrical two-phase induction motor in stationary frame can be defined as

$$v_{s\alpha} = R_{s\alpha} i_{s\alpha} + \frac{d\psi_{s\alpha}}{dt} \tag{1}$$

$$v_{s\beta} = R_{s\beta} i_{s\beta} + \frac{d\psi_{s\beta}}{dt} \tag{2}$$

$$v_{r\alpha} = 0 = R_{r\alpha} i_{r\alpha} + \frac{d\psi_{r\alpha}}{dt} + a\omega_r \psi_{r\beta} \tag{3}$$

$$v_{r\beta} = 0 = R_{r\beta} i_{r\beta} + \frac{d\psi_{r\beta}}{dt} + a\omega_r \psi_{r\alpha} \tag{4}$$

where the stator and rotor flux linkages can be defined as

$$\psi_{s\alpha} = L_{s\alpha} i_{s\alpha} + L_{m\alpha} i_{r\alpha} \tag{5}$$

$$\psi_{s\beta} = L_{s\beta} i_{s\beta} + L_{m\beta} i_{r\beta} \tag{6}$$

$$\psi_{r\alpha} = L_{m\alpha} i_{s\alpha} + L_{r\alpha} i_{r\alpha} \tag{7}$$

$$\psi_{r\beta} = L_{m\beta} i_{s\beta} + L_{r\beta} i_{r\beta} \tag{8}$$

where $v_{s\alpha}$, $v_{s\beta}$, $v_{r\alpha}$, $v_{r\beta}$ are the α-β stator and rotor voltages respectively, $i_{s\alpha}$, $i_{s\beta}$, $i_{r\alpha}$, $i_{r\beta}$ are the αβ stator and rotor currents, $\psi_{s\alpha}$, $\psi_{s\beta}$, $\psi_{r\alpha}$, $\psi_{r\beta}$ are the αβ stator and rotor flux linkages, $R_{s\alpha}$, $R_{s\beta}$, $R_{r\alpha}$, $R_{r\beta}$ are the stator and rotor resistances, $L_{s\alpha}$, $L_{s\beta}$, $L_{r\alpha}$, $L_{r\beta}$ are the stator and rotor inductances, $L_{m\alpha}$, $L_{m\beta}$ are the mutual inductances, ω_r is the electrical rotor angular speed, d/dt is the differential operator and a is the turns ratio between the main and auxiliary windings.

B. Control methods

1) Method I: using three PI controllers

A simple method to control the current is using a closed loop with PI controller in the stationary frame. Since the two-phase induction motor is fed by a conventional three-leg inverter, three closed loops with PI controllers are used. The essential structure of the current regulated two-phase AC system, driven from a conventional three-leg voltage source inverter is shown in Fig. 2. The voltage source inverter topology is the same as a conventional three phase bridge inverter, consisting of six IGBT and diodes, supplying a two-phase induction motor, where the main winding and auxiliary winding, connected to the three-leg inverter represent the load of both phase A and phase B.

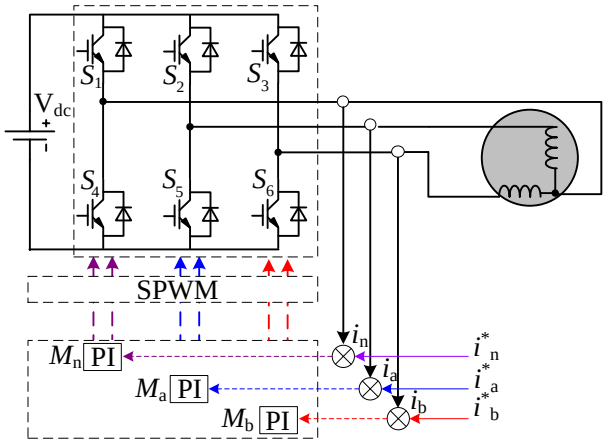

Fig. 2. Block diagram of 3 PI control.

However, since the output currents of three legs are not independent from each other, this method needs to be improved to achieve good performance.

2) Method II: using two PI controllers

It can be noted that the floating neutral leg has only 2 degrees of freedom. In [11] only two PI controllers are required and the command signal for the third leg is generated based on the other two regulated phases according to

$$M_n = -M_a - M_b \tag{9}$$

where M_a, M_b, M_n are the command signal for phase A and phase B and the neutral leg respectively, as shown in Fig. 3. However, since this is an unbalanced three phase system the phase voltage of the third leg is zero for a TPIM, (1) does not apply to this topology. Also, a PI controller can not eliminate the steady-state error to zero on AC quantities since it can not achieve an infinite forward gain.

3) Proposed method

As shown above that there are disadvantages of both method I and method II, a novel method modulating the potential of neutral leg middle point based on its average switching state equations with a proposed algorithm and using two closed loops with an optimized PR controller is introduced.

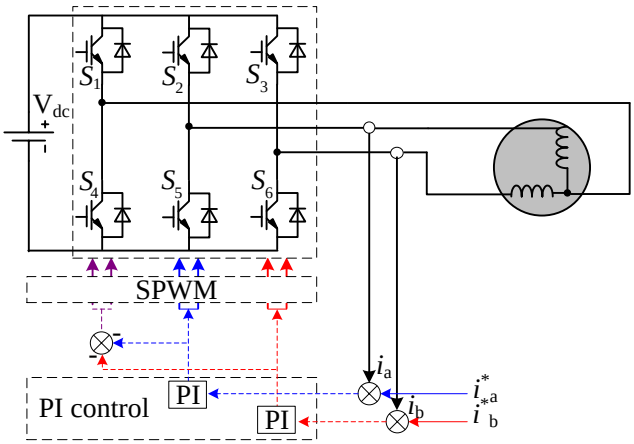

Fig.3. Block diagram of conventional 2 PI control.

From Fig. 1, it is clear that

$$n_A = S \bullet V_{dc},\ n_B = S \bullet V_{dc},\ n_N = S \bullet V_{dc} \tag{10}$$

S=1 when the upper switch of each leg is on, and S=0 when it is off. Furthermore, n_A, n_B, n_N are the potential of points A, B, N respectively as shown in Fig. 1, referring to the negative side of the DC bus voltage source. Then the average value of n_A, n_B, n_N in a switching period can be expressed as

$$\langle n_A \rangle_{T_S} = \langle S \rangle_{T_S} \bullet V_{dc} \tag{11}$$

$$\langle n_B \rangle_{T_S} = \langle S \rangle_{T_S} \bullet V_{dc} \tag{12}$$

$$\langle n_N \rangle_{T_S} = \langle S \rangle_{T_S} \bullet V_{dc} \tag{13}$$

While

$$\langle S \rangle_{T_S} = D(T) = \frac{1}{2}(1 + m \sin \omega t) \tag{14}$$

then

$$\langle n_A \rangle_{T_S} = \frac{1}{2} V_{dc}(1 + m \sin \omega t) \tag{15}$$

Assume that

$$\begin{aligned} \langle n_B \rangle_{T_S} &= \frac{1}{2} V_{dc}\left(1 + m \sin(\omega t + \alpha)\right) \\ \langle n_N \rangle_{T_S} &= \frac{1}{2} V_{dc}\left(1 + m \sin(\omega t + \beta)\right) \end{aligned} \tag{16}$$

Then based on the fact that the phase shift between two phases of a two-phase induction motor is 90°, the average value of phase A and phase B voltage in a switching time period can be expressed as

$$\begin{aligned} \langle U_a \rangle_{T_S} &= \langle n_A \rangle_{T_S} - \langle n_N \rangle_{T_S} = mV_{dc} \sin(-\frac{\beta}{2}) \cos(\omega t + \frac{\beta}{2}) \\ \langle U_b \rangle_{T_S} &= \langle n_B \rangle_{T_S} - \langle n_N \rangle_{T_S} = -mV_{dc} \cos(-\frac{\beta}{2}) \sin(\omega t + \frac{\beta}{2}) \end{aligned} \tag{17}$$

From the equations mentioned above, assume that

$$\max[n_A, n_B] + \min[n_A, n_B] = X, 0 \le X \le 2V_{dc} \tag{18}$$

where X is defined as (18), which can be written as

$$\max[U_a + n_N, U_b + n_N] + \min[U_a + n_N, U_b + n_N] = X \tag{19}$$

Then n_N can be solved as

$$n_N = \frac{1}{2}(X - \max(U_a, U_b) - \min(U_a, U_b)) \tag{20}$$

The value of X has influence on the performance of this control system, and the most convenient way to find proper value of X is increasing the value of it step by step and observing the step response of the current control loop on simulation model and real experiment system. Assume that the output of two PR controllers of phase A and phase B are v_x, v_y respectively. Then the modulating signal for the three legs can be obtained as

$$\begin{aligned} M_a &= v_x + n_N \\ M_b &= v_y + n_N \\ M_n &= n_N \end{aligned} \tag{21}$$

which act as the modulation signals of SPWM to compare with the triangular carrier wave to produce command signals for switches as shown in Fig. 4. The curve of THD referring to the value of X is shown in Fig. 5. It can be observed that the value of THD decreases as X increases at the beginning, but it increases as X increases after a certain point. Thus the value of X can be determined.

As proposed and introduced in [8] [13], a significant feature of PR controller is its ability to track sufficiently the AC current and achieving the zero steady-state error at the certain resonant frequencies. An ideal PR controller in the s-domain can be defined as

$$G_r(s) = K_p + \frac{K_r s}{s^2 + \omega_0{}^2} \tag{22}$$

where K_p is the proportional gain and K_r denotes the resonant gain. However, it is difficult to implement an ideal PR controller practically in DSP using a fixed point calculation. Thus the practical expression of PR controller can be obtained as

$$G_r(s) = K_p + \frac{K_r s}{s^2 + \omega_r s + \omega_0{}^2} \tag{23}$$

where ω_r is the resonant cut off frequency. It can be seen from the expression that infinite forward controller gain can be achieved by the denominator at some certain values. The controller parameters can be determined by first maximizing K_p while achieving unity loop gain with a required phase margin (40°~60°) at the maximum possible crossover frequency and then maximizing the K_r.

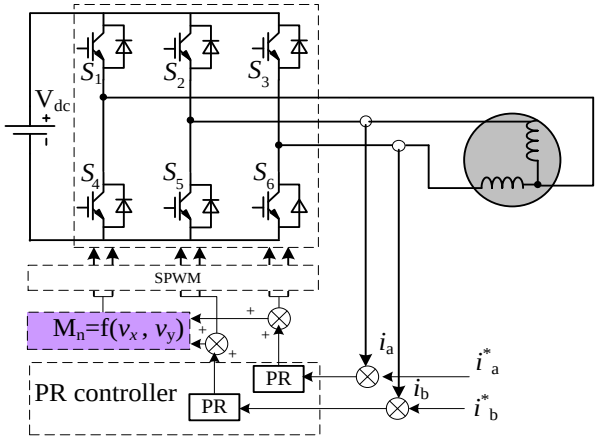

Fig. 4. Block diagram of proposed control.

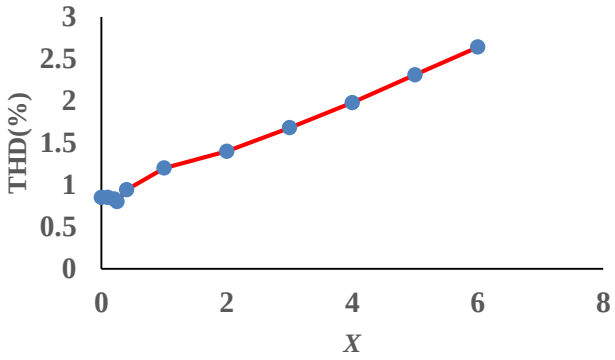

Fig. 5. Curve of THD referring to *X*.

C. Simulation Results

The parameters of the current regulation system is shown in TABLE I. The simulation results, output currents of phase A and phase B as well as the error between them with reference signals, of all three methods are shown in Fig. 6, Fig. 7 and Fig. 8. And TABLE II. shows the THD and peak overshoot of all methods. It can be seen that the curve of errors of method I, method II, method III is becoming thinner, indicating that method III can achieve a better performance than method I, method II since the coupling between three legs are avoided, error caused by imbalance can be eliminated by modulating the potential of neutral leg middle point and PR controller performs more effective on AC quantity.

TABLE I. PARAMETERS OF THE AC SYSTEM

Circuit parameters	Value
Resistive component of load R_a(Ω)	4.56
Inductive component of load L_a(mH)	27.14
Resistive component of load R_b(Ω)	5.982
Inductive component of load L_b(mH)	24.35
DC bus voltage(V)	311
Back EMF frequency(Hz)	50
Switching frequency(Hz)	3000

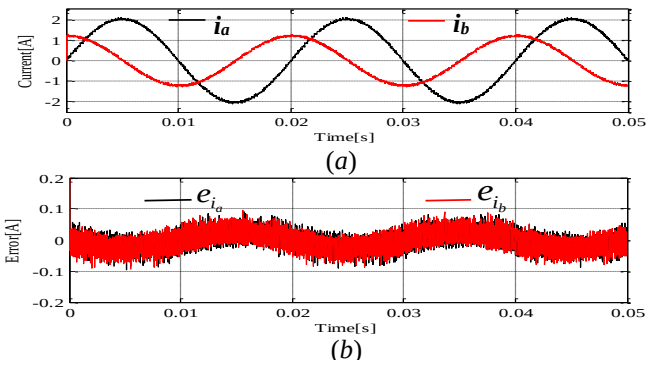

Fig. 6. Output currents and errors of method I, (a), output currents, (*b*), errors.

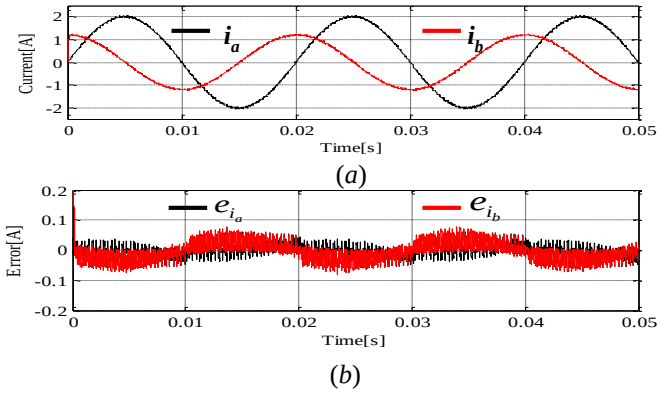

Fig. 7. Output currents and errors of method II, (a),output currents, (*b*), errors.

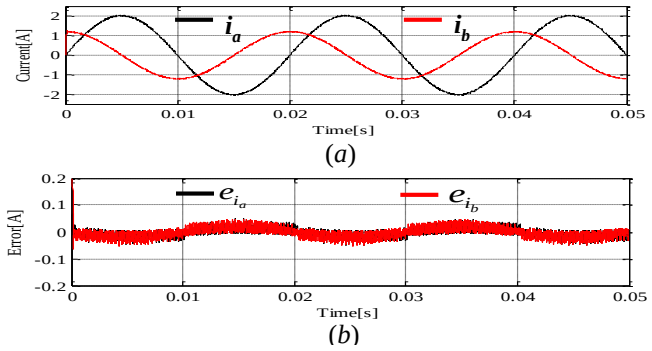

Fig. 8. Output currents and errors of method III, (a), output currents, (*b*), errors.

TABLE II. COMPARISON BETWEEN ALL THREE METHODS

	THD	Peak overshoot
Method I	1.4%	0.07
Method II	1.31%	0.05
Method III	0.78%	0.04

Where i_a is the output current of phase A, i_b is the output current of phase B, e_{ia} is the error between the output current and reference of phase A, e_{ib} is the error between the output current and reference of phase B.

D. Experiment Results

In order to demonstrate the effectiveness of the proposed control algorithm, an experimental prototype has been implemented. The diagram of the hardware system shown in Fig. 9 includes a main power circuit, a current detecting circuit, as well as TMS320F28335. Also a 0.75 kW single phase (unbalanced two phase) induction motor was used as an unbalanced two phase induction machine connecting directly to the VSI. Also, the PR controller is discretized by bilinear transformation to implement on DSP. The output currents are shown in Fig. 10, Fig. 11 and Fig. 12.

Fig. 9. Diagram of the hardware system.

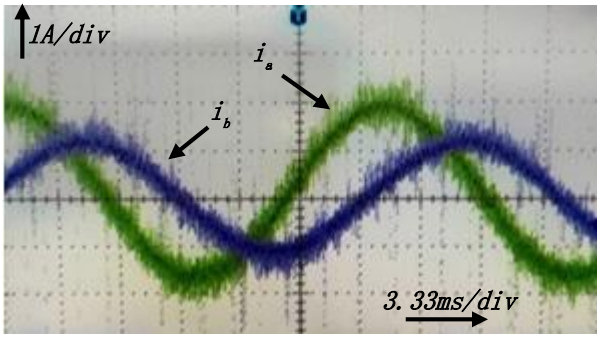

Fig. 10. Output currents of method I.

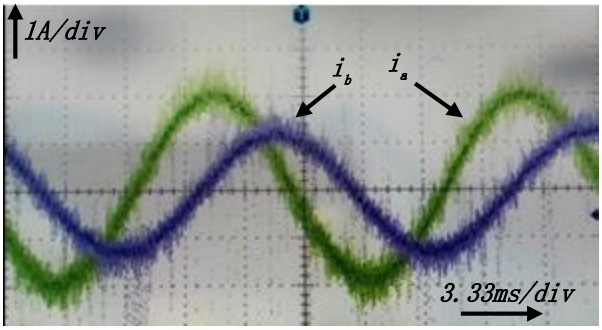

Fig. 11. Output currents of method II.

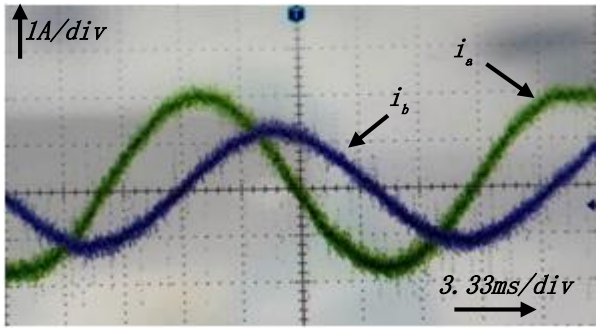

Fig. 12. Output currents of method III.

From the experiment results above, it can be easily noticed that the current ripple introduced by method I and method II are greater than that introduced by the proposed method, indicating that the proposed algorithm can achieve a better performance on eliminating the error between the output current and reference current, which are consistent with the simulation results.

III. Conclusion

A conventional three-leg voltage source inverter is used for controlling the current of a two-phase induction motor in this paper. Two conventional control strategies, using two or three closed loop PI controllers which also works for three-phase load in the stationary frame, is introduced. A novel control method, using two closed loops with PR controller and a new algorithm modulating the potential of the neutral leg middle point is then proposed. All methods are verified in MATLAB/SIMULINK, as well as by experiment, which demonstrates that the proposed control method can achieve a better performance in terms of THD, peak overshoot.

References

[1] C.-M. Young, C.-C. Liu, and C.-H. Liu, "New inverter driven design and control method for two-phase induction motor drives," Inst. Elec.Eng. Proc. Electric Power Applicat., vol. 143, no. 6, pp. 458–466, Nov.1996.

[2] E. R. Benedict and T. A. Lipo, "Improved PWM modulation for a permanent-split capacitor motor," in Proc. IEEE Ind. Appl. Conf., 2000, vol. 3, pp. 2004-2010

[3] F. Blaabjerg, F. Lungeanu, K. Skaug, and M. Tonnes, "Two-phase induction motor drives," IEEE Ind. Applicat. Mag., July-Aug. 2004

[4] Jang, Do-Hyun. "PWM methods for two-phase inverters." Industry Applications Magazine, IEEE 13.2 (2007): 50-61.

[5] D. G. Holmes and A. Kotsopoulos "Variable speed control of single and two phase induction motors using a three phase voltage source inverter", IEEE Industrial Applications Society annual meeting conference records, pp.613 -620 1993

[6] M. B. de R. Correa, C. B. Jacobina, A. M. N. Lima, and E. R. C. da Silva, "A three-leg voltage source inverter for two-phase ac motor drive system", Proc. IEEE PESC',01, vol. 3, pp.1458 -1463 2001

[7] M. P. Kazmierkowski and L. Malesani, "Current control techniques for three-phase voltage-source PWM converters: A survey", IEEE Trans. Ind. Electron., vol. 45, pp. 691 -703 1998

[8] Hsu, Ping, and Michael Behnke. "A three-phase synchronous frame controller for unbalanced load [invertor operation]." Power Electronics Specialists Conference, 1998. PESC 98 Record. 29th Annual IEEE. Vol. 2. IEEE, 1998.

[9] Phan, Van-Tung, and Hong-Hee Lee. "Enhanced proportional-resonant current controller for unbalanced stand-alone DFIG-based wind turbines." Journal of Electrical Engineering & Technology 5.3 (2010): 443-450.

[10] D.N. Zmood, D.G. Holmes, "Stationary frame current regulation of PWM inverters with zero steady-state error" IEEE Trans. on Power Electr. Vol. 18, pp. 814-822, May 2003.

[11] W. Y. Kong , D. G. Holmes and B. P. McGrath "Enhanced three phase ac stationary frame PI current regulators", Proc. IEEE ECCE, pp.91 -98 2009

[12] W. Y. Kong , D. G. Holmes and B. P. McGrath "Improved stationary frame AC current regulation using feedforward compensation of the load EMF", Proc. IEEE APEC-09, IEEE Appl. Power Electron. Conf., pp.145 -151

[13] B. P. McGrath , S. G. Parker and D. G. Holmes "High-performance current regulation for low-pulse-ratio inverters", IEEE Trans. Ind. Appl., vol. 49, no. 1, pp.149 -158, 2013